Carbohydrate Polymers 88 (2012) 992–1001

Contents lists available at SciVerse ScienceDirect

Carbohydrate Polymers

journal homepage: www.elsevier.com/locate/carbpol

Synthesis of TiO_2–SiO_2 colloid and its performance in reactive dyeing of cotton fabrics

Darinka Fakin[a], Nika Veronovski[b], Alenka Ojstršek[a], Mojca Božič[a,*]

[a] Institute for Engineering Materials and Design, University of Maribor, Smetanova ul. 17, SI-2000 Maribor, Slovenia
[b] Cinkarna, Metallurgical and Chemical Industry Celje, Inc., Kidričeva 26, SI-3001 Celje, Slovenia

ARTICLE INFO

Article history:
Received 2 December 2011
Received in revised form 13 January 2012
Accepted 17 January 2012
Available online 24 January 2012

Keywords:
TiO_2 nanoparticles
Surface treatment
Cellulose
Reactive dyeing
UV protection

ABSTRACT

Newly synthesized SiO_2 surface treated TiO_2 nanoparticles (TiO_2–SiO_2) were prepared, characterized and utilized in functional dyeing as combined reactive dyeing of cotton fabrics. Factors affecting the dyeing and functional properties of the treated fabric, concentration of TiO_2–SiO_2 and of reactive dye as well as dyeing regime were studied. The chemical and morphological structures of nano-upgraded cotton fabrics were characterized by ATR-FTIR spectroscopy and scanning electron microscopy. UV-blocking ability, coloration and comfortable behavior of cotton have been evaluated through ultraviolet protection factor, CIE $L^*a^*b^*$ color values and air permeability determinations, respectively. Incorporation of TiO_2–SiO_2 into the dyeing with reactive dyes brought about an outstanding UV protection functionality of the dyed fabrics even after 15 laundering cycles with a negligible negative impact on color and comfortable properties. Improvement or decrement in the UV protection, comfort, and dyeing properties is governed by the reactant concentrations and the dyeing temperature.

1. Introduction

In recent years, there has been a progressive increase in UV radiation on human skin caused by the depletion of the ozone in the earth's atmosphere. The United States Environmental Protection Agency estimates that ozone depletion will lead to between three and fifteen million new series of negative health effects such as acceleration of skin ageing, photodermatosis (acne), erythema (skin reddening), and severe skin cancer by the year 2075 (Ajoy, 2004; Wang & Hauser, 2010). Therefore there is strong demand of providing protection from UV, where textiles play an important role.

Cellulosic fabrics, i.e. cotton, linen and viscose are widely used and have outstanding characteristics such as non-toxicity, biocompatibility, high water absorbency and moisture, being safe–comfortable to wear and easy to dye. For these reasons, the apparel industry is predominantly cotton based, and the share of cotton in total fiber consumption is about 50% (Aiqin, Yanhong, & Huawei, 2010; El Shafie, Fouda, & Hashem, 2009; Tavčer, 2010). Cellulosic fabrics, especially viscose fabrics made from filament yarns, are ideal for summer clothing. However, an average weight cotton summer clothes offer only low ultraviolet protection factor (UPF), i.e. less than 15 (Xin, Daoud, & Kong, 2004), but the sufficient UPF for clothing should be 40–50+. These UPF values qualify the fabric as UV-protective and allow the manufacturer to make a claim in the marketplace.

Nanotechnology offers high potential to create new materials with applications in medicine, electronics, energy production, and lately for functional textiles (Zhang, Wu, Chen, & Wu, 2010). Titanium dioxide (TiO_2) has attracted significant attention in the past decades because of its excellent physicochemical properties, non-toxicity and good heat resistance. Current research on TiO_2 is focused on the photocatalytic property for the development of photocatalysts, semiconductors in solar cells and UV absorbance property for the protection of materials from UV damage (Dastjerdi & Montazer, 2010; Dastjerdi, Montazer, & Shahsavan, 2010; Veronovski, Andreozzi, La Mesa, & Sfiligoj-Smole, 2010; Veronovski, Sfiligoj-Smole, & Viota, 2010). Up to now, there have been studies already reported on utilizing TiO_2 as UV protector, either in the form of pure inorganic coatings or embedded in polymer matrices in the form of hybrid materials. However, despite TiO_2 shows good UV-shielding property, it also exhibits strong photocatalytic behavior when absorbing UV rays, which is harmful for the photostability of polymer matrices and substrates (Yang, Zhu, & Pan, 2004). Recently, to suppress the photocatalytic property of TiO_2 while retaining its UV-protective properties, inert shells, which usually composed of silica (SiO_2), alumina (Al_2O_3), cerium (CeO_2), magnesia (MgO), zirconia (ZrO_2), yttrium (Y_2O_3), etc., their mixtures or a various polymers were coated onto TiO_2 cores (Cui, Zayat, Parejo, & Levy, 2008). Those treatments are most commonly precipitated in layers offering desired coat formation. For the preparation of the optimal TiO_2–SiO_2 and other

* Corresponding author. Tel.: +386 2 220 7924; fax: +386 2 220 7990.
E-mail address: mojca.bozic@uni-mb.si (M. Božič).

0144-8617/$ – see front matter © 2012 Elsevier Ltd. All rights reserved.
doi:10.1016/j.carbpol.2012.01.046

core–shell particles, there are still some limitations. Firstly, stable TiO_2 colloids or TiO_2 dispersion has to be prepared prior to the silica coating process. Secondly, SiO_2 layer is usually derived in non-aqueous environment, which needs excess use of potentially harmful organic solvent. Thirdly, core–shell particles synthesized are relatively large because of the agglomeration of commercial TiO_2 powders (Veronovski, Andreozzi, et al., 2010; Veronovski, Sfiligoj-Smole, et al., 2010; Zhang et al., 2010). Thus, how to minimize agglomeration and to obtain uniform SiO_2 layers in aqueous environment remains an aspect that needs to be addressed before these kinds of product become commercialized.

The present research article involves two major objectives: (i) the use of low-cost and non-hazardous chemicals and development of a rapid, versatile, controllable, reproducible approach to synthesize stable suspensions of SiO_2 surface treated rutile TiO_2 nanoparticles; and (ii) feasibility of carrying out combined cellulose reactive dyeing (Bezaktiv Red S-3B 150) with TiO_2–SiO_2 application in one step. More specifically, the present work is undertaken with a view to develop a novel one-bath exhaustion process for combined TiO_2–SiO_2 reactive dyeing to obtain superior UPF of cotton fabric for summer cloths as well as maximal fastness properties during usage and care.

To achieve the goal, cotton fabrics were subjected to different dye and TiO_2–SiO_2 nanoparticle concentrations at various dyeing temperatures with a view to determine the best formulation along with optimum conditions that can be applied to cotton fabrics and provoke higher fabric performance. The efficiency of one-step process for TiO_2–SiO_2 reactive dyeing was evaluated monitoring the dyeing properties of cotton fabric for color yield (K/S) and the colorimetric data of CIE $L^*a^*b^*$ as well as properties such as air permeability and UPF factor of treated samples. Furthermore, to study nanocoating formation, investigated properties were size, form, and electro-kinetic characteristics of bulk and embedded TiO_2 nanoparticles as well as the morphology and properties of the coatings applied to the cellulose substrate.

2. Experimental

2.1. Materials

Industrially bleached (prepared for dyeing) plane-wave 100% cotton fabric with a mass of 139 g/m^2, warp density of 26 threads/cm and weft density of 21 threads/cm, and warp fineness of 27.4 tex and weft fineness of 33 tex was used in the experiments.

Bifunctional reactive dye namely Bezaktiv Red S-3B 150 (Bezema) and levelling agent Meropan OFS (Bezema) were of commercial grade.

For the preparation of SiO_2 surface treated TiO_2 nanoparticles the following chemicals were used: suspension of TiO_2 nanoparticles in the rutile crystalline form (produced by Cinkarna Celje using sulfate synthesis process), sodium silicate, sodium hydroxide, sulfuric acid, hydrochloric acid and deionized water.

All other chemicals used during this study were of laboratory reagent grade.

2.2. Methods

2.2.1. Synthesis of TiO_2–SiO_2 nanoparticles

The synthesis of TiO_2–SiO_2 was performed according to the Patent Application no. P-201000397 (Veronovski, Verhovšek, & Selišnik, 2011) with slight modification. Briefly, suspension of nano TiO_2 in rutile crystalline form used in this research contained approximately 20% solid material. The nanoparticle coating was accomplished by precipitating white hydrated oxides onto the TiO_2 surface using a wet precipitation process. Rutile was subsequently surface treaded with hydrated amorphous SiO_2. As a precursor, sodium silicate was used. Gradually, 3 wt% SiO_2 precipitated onto TiO_2 surface.

2.2.2. Dyeing

The dyeing with reactive dye Bezaktiv Red S-3B 150, combined with TiO_2–SiO_2 nanoparticles was accomplished according to one-bath exhaustion procedure using liquor ratio of 1:20 in a sealed, stainless-steel dye-pot of 250 cm^3 capacity, housed in a Turby (W. Mathis) dyeing apparatus with high bath circulation. The cotton fabric samples were immersed in a dye bath composed of the Bezaktiv Red S-3B 150 (0.5, 1.0 or 1.5% of weight of fabric (owf)), NaCl (30, 40 or 45 g/L), $NaHCO_3$ (5 g/L) and 32% NaOH (0.8, 1.2 or 1.6 mL/L). All dyeing experiments were carried out with TiO_2–SiO_2 addition (1, 2 or 3% owf) at temperatures of 60, 80 and 100 °C for 110 min. Typical formulations used in this study are given in the text. After 40 min of dyeing at given temperature, initial amount of NaOH was added again, and dyeing continued for 70 min. Thereafter, cotton fabrics were removed from the dye-bath and rinsed thoroughly in tap water. To remove unfixed reactants, samples were wetted at 50 °C for 5 min in the presence of 1 g/L Na_2CO_3 and 2 g/L nonionic wetting agent, rinsed in tap water and finally air dried.

2.2.3. Washing procedure

Wash fastness of the TiO_2–SiO_2 coatings on a cotton fabric was determined according to the standard ISO 105-C06 in a Mathis Labomat. The coated fabric samples were washed repetitively up to 15 times; the duration of the washing cycles was 30 min and was carried out in a solution of SDC standard detergent of concentration 4 g/L, previously heated to 40 °C, to give a liquor ratio of 50:1. After washing, the samples were rinsed several times in distilled water and then held in cold tap water for 30 min, squeezed and dried at room temperature. The quality of the coatings was assessed with UPF measurements after the first, fifth, tenth and fifteenth washing cycles.

2.3. Analytical procedures

2.3.1. Surface morphology determination – SEM and TEM

Scanning electron microscopy (SEM) and transmission electron microscopy (TEM) were utilized for surface treated nano TiO_2 morphology analysis. In addition to that, a microscopic evaluation of the morphological changes occurring after the dyeing treatment of cotton samples was carried out using a Zeiss SIGMA VP SEM.

A drop of TiO_2 suspension was dropped on the adhesive carbon band on brass holders for the observation on a Zeiss SIGMA VP scanning electron microscope (Carl Zeiss NTS GmbH, Germany), with a maximum resolution up to 1.5 nm at 20 kV. In the case of dyed cotton samples with TiO_2–SiO_2, approximately 1 cm^2 of the fabric was attached on the adhesive carbon band on brass holders. SEM images were collected and elaborated according to standard procedures.

In addition, morphology analysis of surface treated nano TiO_2 was performed using transmission electron microscope (TEM, JEOL 2100F, Japan). For the analysis, a drop of TiO_2 suspension was dropped on Cu-grid.

2.3.2. Determination of electrochemical properties

Mütek^{TM} PCD-04 Particle Charge Detector (BTG Instruments GmbH, Germany) in combination with an external titrator, e.g. 905 Titrando (Metrohm, Switzerland) was used for charge identification of aqueous samples and for determining their isoelectric point (IEP).

2.3.3. Color and color fastness evaluations

The color of the dyed fabrics with and without TiO_2–SiO_2 was estimated from reflectance measurements using a Spectraflash SF 600 PLUS spectrophotometer (Datacolor) at standard illuminant D65 (LAV/Spec. Incl., d/8, D65/10°).

The color was evaluated in terms of the CIE $L^*a^*b^*$ color system, where L^*, a^* and b^* are the coordinates of the color in the mathematical combination of Cartesian and cylindrical coordinate system, based on the theory that color is perceived as L^* (lightness, which varies from 100 for a perfect white to 0 for absolute black), a^* (which varies from greenness to redness), and b^* (which varies from blueness to yellowness, from negative to positive values). Other optical parameters used were color saturation (C^*) and hue representing the color tone (h), and a color depth (K/S) calculated from the Kubelka–Munk equation (Božič, Díaz-González, Tzanov, Guebitz, & Kokol, 2009):

$$\frac{K}{S} = \frac{(1-R)^2}{2R} \tag{1}$$

where K is the absorption coefficient, S is the light-scattering coefficient and R is the reflectance of the fiber at a wavelength of maximum absorption (540 nm). On the basis of the measured CIE $L^*a^*b^*$ color coordinates, the color difference (ΔE^*) was determined as:

$$\Delta E^* = \sqrt{(\Delta a^*)^2 + (\Delta b^*)^2 + (\Delta L^*)^2} \tag{2}$$

where ΔL^*, Δa^* and Δb^* are the difference between the treated (dyed fabric with TiO_2–SiO_2) and the control (dyed without TiO_2–SiO_2) cotton samples. The values represent an average of three reflectance measurements, taken at different positions on the dyed fabric, which was folded twice in order to get four thicknesses.

Color fastnesses to light were determined by the standard ISO 150-B04 using a XENOTEST 150S (Heraeus) with a Xenon light source at an irradiance of 1154 W/m^2 for 15 h.

2.3.4. Attenuated total reflectance infrared spectroscopy (ATR-FTIR)

The spectra of the dyed cotton samples with and without TiO_2–SiO_2 were recorded using a Perkin-Elmer Spectrum One FTIR spectrometer with a Golden Gate ATR attachment and a diamond crystal. The absorbance measurements were carried out within the range of 650–4000 cm^{-1}, with 16 scans and a resolution of 4 cm^{-1}. The ATR-FTIR spectra were normalized to the absorption band at 1200 cm^{-1}, which is unaffected by the environmental changes (Hulleman, Hazendonk, & Dam, 1994).

2.3.5. Air permeability

Air permeability measurements were carried out according to the SIST EN ISO 9237:1999 Standard by means of Karl Schröder KG apparatus. From the amount of air passing through the sample under a pressure of 20 mm H_2O, the air permeability was determined as Q given by:

$$Q = \frac{q}{6a} \tag{3}$$

where q is the volume of air flowing through the sample of area, a, expressed in L/h and Q is the volume of air in m^3 passing through 1 m^2 of the fabric per minute at the required pressure. The results represent the mean values of 5 measurements.

2.3.6. UV-protection factor (UPF)

UPF values were assessed according to the Australian/New Zealand Standard (AS/NZS 4399-1996), over the ultraviolet spectral region of wavelength 290–400 nm using a solarscreen 50 spectrophotometer (Varian) fitted with an integrating sphere accessory and a fabric holder accessory. UPF of each sample is calculated according to the following equation:

$$\mathrm{UPF}_i = \frac{\sum_{\lambda=290}^{400} E_\lambda S_\lambda \ \Delta\lambda}{\sum_{\lambda=290}^{400} E_\lambda S_\lambda T_\lambda \ \Delta\lambda} \tag{4}$$

where E_λ is the CIE relative erythermal spectral effectiveness; S_λ is the solar spectral irradiance; T_λ is the spectral transmittance of the fabric; $\Delta\lambda$ is the wavelength step in nm and λ is a wavelength in nm.

The rated UPF of the sample is calculated introducing a statistical correction. Starting from the standard deviation of the mean UPF, the standard error in the mean UPF is calculated for a 99% confidence level. The rated UPF will be the mean UPF minus the standard error, rounded down to the nearest multiple of five. According to the Australian classification scheme, fabrics can be rated as providing good, very good, and excellent protection if their UPF values range from 15 to 24, 25 to 39 and above 40, respectively. For UPF ratings of 55 or greater, the term 50+ shall be used.

$$\mathrm{UPF} = \overline{\mathrm{UPF}} - t_{\alpha/2,N-1} \cdot \frac{SD}{\sqrt{N}} \cdots \tag{5}$$

where $\overline{\mathrm{UPF}}$ is the mean UPF; $t_{\alpha/2,N-1,t}$ is the variate for a confidence level $\alpha = 0.005$ and SD is the standard deviation of the mean UPF.

3. Results and discussion

3.1. Synthesis and characterization of TiO_2–SiO_2 nanoparticle suspensions

It is well known that rutile is less photochemically active than anatases (Bozzi, Yuranova, & Kiwi, 2005), therefore, rutile form of TiO_2 was chosen and modified with SiO_2 to further suppress photochemical activity towards the textile substrate upon light irradiation. Additionally, bondability of TiO_2 on cotton fabrics was increased with SiO_2 as chemical spacers between TiO_2 and cellulosic fibers.

Coating the TiO_2 nanoparticles was accomplished by precipitating white hydrated SiO_2 onto the TiO_2 surface. Precipitation process is strongly influenced by the reaction conditions (e.g. pH, temperature, reagents, and order of addition), thus, affecting final product characteristics (Viravathana & Marr, 2000). SiO_2 deposition under acid or neutral pH medium yields submicroscopic particles joined together in a gel-like structure, resulting in "fluffy" coating, providing better spacing and optical efficiency. On the other hand, SiO_2 deposition under basic pH medium results in a dense, glassy shell that encapsulates the particle and provides the highest durability available. Synthesized suspension of SiO_2 coated TiO_2 nanoparticles yielded neutral pH character therefore presenting un-harmful media to cellulose-based materials.

SEM and TEM were used to characterize the morphology of SiO_2 layer formed on the TiO_2 surface. SEM image, presented by Fig. 1, shows the SiO_2 coated TiO_2 nanoparticles with uniform distribution without agglomerate formation, while Fig. 2 shows TEM image of untreated and SiO_2 treated non-spherical shaped rutile nanoparticles (ca. 80 nm in length and 25 nm in width). Untreated TiO_2 nanoparticles have sharp edges which became smoother after amorphous SiO_2 precipitation as shown in Fig. 2. SiO_2 layer formed is homogeneous and entirely coats the TiO_2 surface. No agglomerates of TiO_2 nanoparticles can be seen after the surface treatment, which proves the formation of stable colloidal suspension.

SEM and TEM results were verified by electrochemical property determination (Fig. 3). The results indicated that the coated nanoparticles with 3 wt% SiO_2 loading had good dispersion stability in water, which also gave further evidence of complete SiO_2 coating layers formed on TiO_2 nanoparticles. An isoelectric point

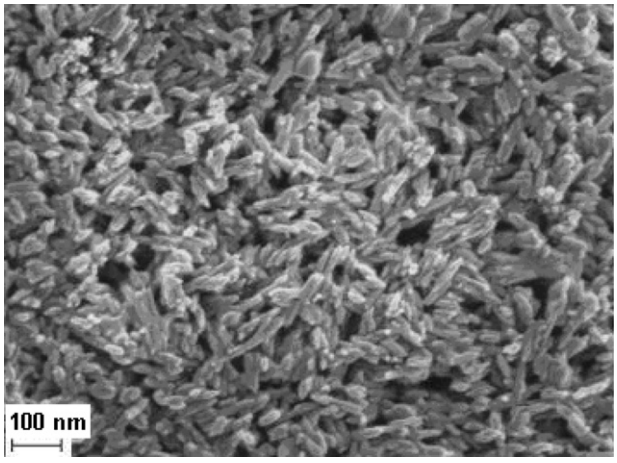

Fig. 1. SEM image of surface treated rutile TiO_2 nanoparticles.

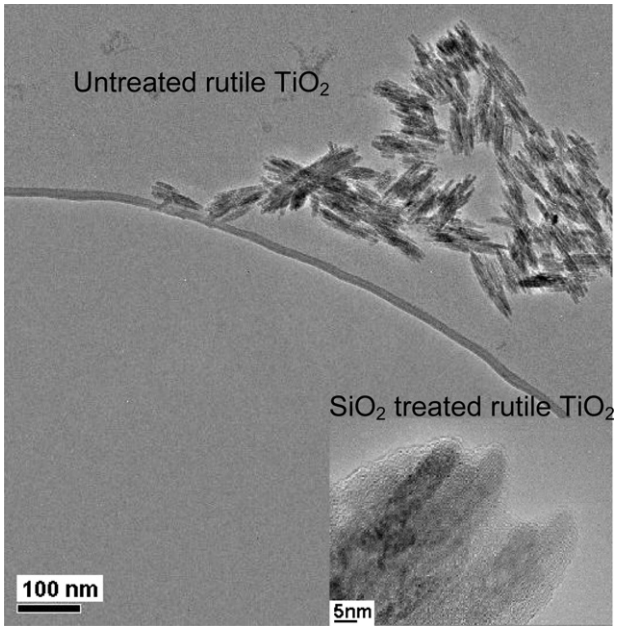

Fig. 2. TEM image of surface treated rutile TiO_2 nanoparticles.

(IEP) values for TiO_2 and SiO_2 coated TiO_2 nanoparticles are shown in Fig. 3. IEP determined for TiO_2 nanoparticle laid around pH 5.5, while SiO_2 layer on the surface of TiO_2 nanoparticles shifted IEP to lower pH values, to pH value ~2. This result is very close to the IEP value of SiO_2 (i.e. 2–3) reported by Parks (1965) and Reed (1995) and proves a successful TiO_2 surface treatment.

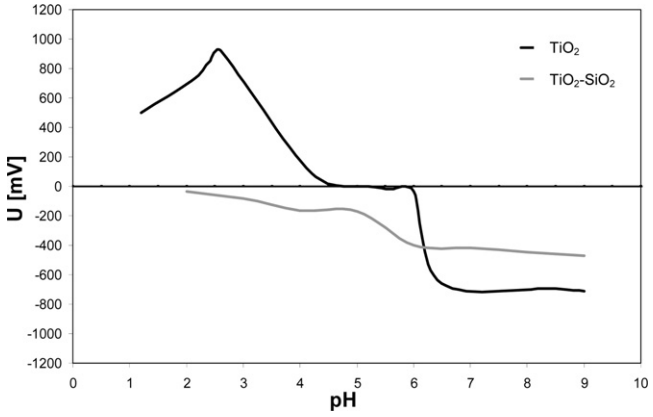

Fig. 3. U-pH function of TiO_2 and SiO_2 coated TiO_2 nanoparticles.

3.2. ATR-FTIR analysis of blank and Bezaktiv Red S-3B 150 – TiO_2–SiO_2 dyed cotton samples

ATR-FTIR difference spectra of blank cotton sample and Bezaktiv Red S-3B 150 dyed cotton samples with different TiO_2–SiO_2 concentrations in the dyeing bath were recorded to identify the structural changes of the dyed samples and to quantify the temperature dependent TiO_2–SiO_2 uptake, as shown in Fig. 4.

Spectrum of blank cotton sample with many free hydroxyl groups on the surface shows characteristic bands at 3500–3200 cm^{-1}, due to O—H valent vibration of water, 2980–2800 cm^{-1}, due to C—H stretching, ~1645 cm^{-1}, due to deformation vibration of water molecules and absorption bands in the 1500–800 cm^{-1} spectral region, which occurred as a result of C—H, O—H, C—O and C—O—C vibrations in glucosidic ring and represents the finger print of cellulose (Ciolacu, Kovac, & Kokol, 2010). The changes of many ATR-FTIR bands characteristic of cotton cellulose reflect the occurrence of the TiO_2–SiO_2 modification through the hydrogen bonds between TiO_2–SiO_2 surface hydroxyl groups and cellulose hydroxyl groups during the reactive dyeing. The presence of TiO_2–SiO_2 on the surface of dyed cotton samples can be seen as an increase in the intensity of absorption bands at 3334 cm^{-1} and 3287 cm^{-1} and is attributed to hydroxyl groups on different sites and to varying interactions between hydroxyl groups on TiO_2, SiO_2 and cellulose (Fig. 4(a)) (Veronovski, Hribernik, Andreozzi, & Sfiligoj-Smole, 2009). Furthermore, band intensities of silica (Si—O—Si linkages), attached on the surface of TiO_2 at 1030, 1055 and 1105 cm^{-1} (Tomšič et al., 2008), and band of Ti—O vibrations at around 980 cm^{-1} increased with increasing content of TiO_2–SiO_2 dyed cotton samples.

Comparing the TiO_2–SiO_2-reactive dyed and blank cotton samples, the appearance of the symmetric O—Ti—O stretch bands at around 667–678 cm^{-1} is evident (Fig. 4(b)). Moreover, the increase of the intensity of these bands with the increase in the TiO_2–SiO_2 concentration, and their shifting to a higher wavenumber, confirmed the structural modification of cellulose structure after TiO_2–SiO_2 bonding.

Here, to quantify how significant the TiO_2–SiO_2 modification was, the intensity ratio of the unaffected OH band at 1200 cm^{-1} and O—Ti—O stretch band at 668 cm^{-1} was evaluated (Table 1). It was found that the ratios A_{668}/A_{1200} increased when compared to the blank cotton sample. Increase was in proportion with increased concentrations of TiO_2–SiO_2. A_{668}/A_{1200} ratios increased from 60 °C to 80 °C of the used dyeing temperature and slightly decreased at 100 °C. A decrease of ratios at boiling point may be related to the increased kinetic energy of the TiO_2–SiO_2 nanoparticles, which causes increasing nanoparticle motion leading to the disrupted hydrogen forces between the nanoparticles and the surface of the fiber. From these results, it can be concluded that the TiO_2–SiO_2 was successfully introduced onto cellulose via hydrogen bonding on the account of the significant increase of the A_{668}/A_{1200} ratio.

3.3. Effect of TiO_2–SiO_2 concentration on the color data of the Bezaktiv Red S-3B 150 cotton dyed samples

A series of cotton samples were dyed via one-bath exhaustion procedure, combined with TiO_2–SiO_2 nanoparticles by varying the dyeing conditions (i.e. temperature), including the amount of the reactive dye and TiO_2–SiO_2 nanoparticles.

Reactive dyes are widely used for dyeing of cellulose as the reactive system enables the dye to covalently bond with the —OH group in cellulose (Ojstršek, Doliška, & Fakin, 2008).

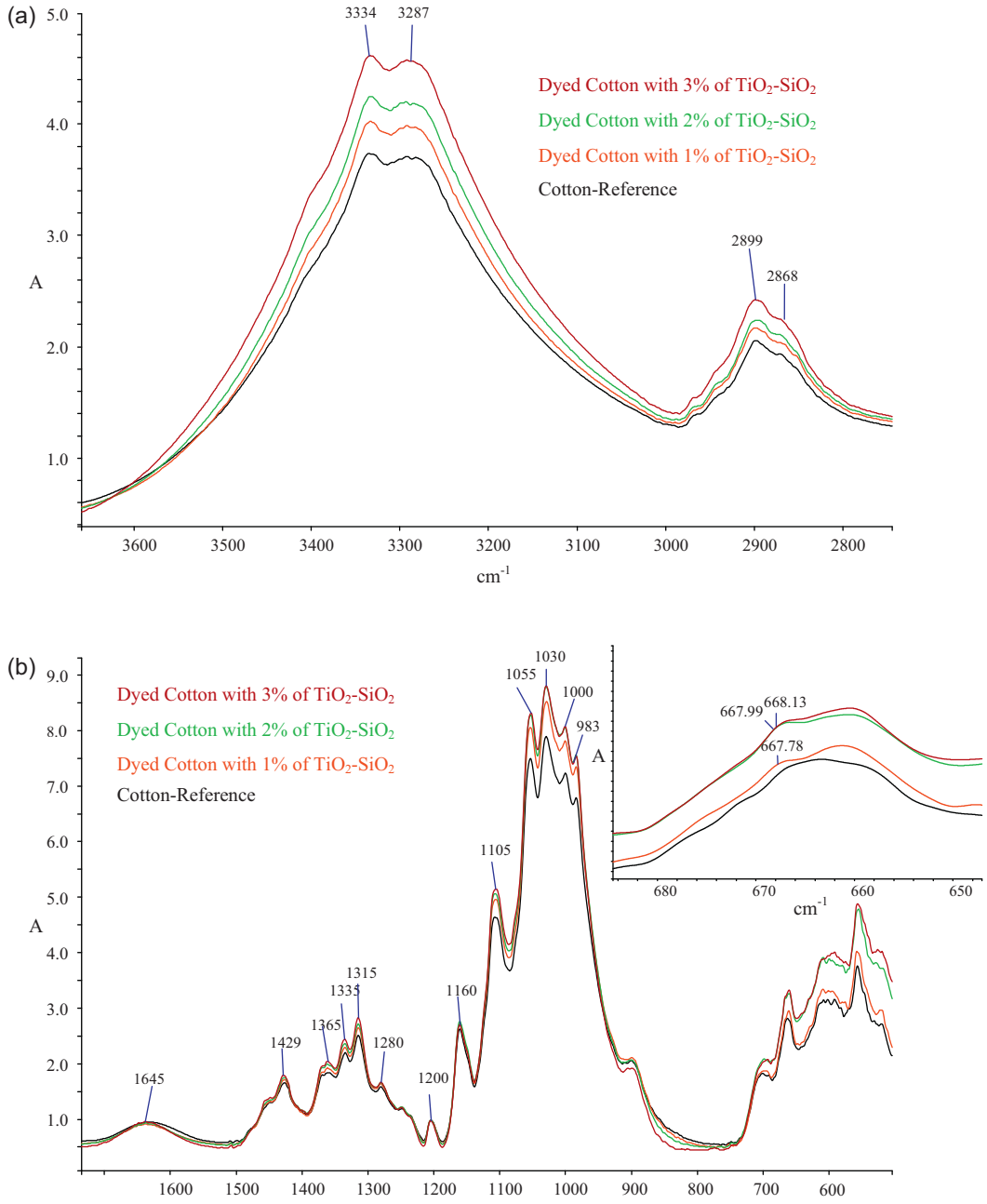

Fig. 4. ATR-FTIR spectra of blank cotton and 0.5% owf Bezaktiv Red S-3B 150 dyed cotton samples, combined with TiO_2–SiO_2 concentration from 1 to 3% owf at 80 °C dyeing temperature.

For the preparation of transparent hybrid materials, smaller inorganic particle and less refractive index difference are preferred (Zhang et al., 2010). The TiO_2 colloidal suspension prepared in our protocol was very small (ca. 80 nm × 25 nm) and the existence of void in the hybrid colloid made the total refractive index of hybrid colloid relatively low. Therefore, according to the CIE $L^*a^*b^*$ color data and UV performance data, transparent UV blocking hybrid coating with negligible effect on the color depth was achieved in this research. The TiO_2–SiO_2 exhaustion and color depth (K/S) values (Table 2) of Bezaktiv Red S-3B 150 dyed cotton samples with different TiO_2–SiO_2 concentrations were in correlation with the quantitatively detected TiO_2 ratios A_{668}/A_{1200} (Table 1). Insignificant (visually undetectable) decrease in color depth due to the presence of TiO_2–SiO_2 can be observed at all TiO_2–SiO_2 concentrations and dyeing temperatures (Table 2). Furthermore, K/S values decreased from 1% to 3% owf of used TiO_2–SiO_2 concentration. Nevertheless, the extent of the decrease was the highest at 60 °C and the lowest at 100 °C indicating different TiO_2–SiO_2 coating morphologies (Fig. 5) affecting the color depth. The obtained color changes could not be visually detected since the values of the color difference (ΔE^*) were around one when using 1% owf TiO_2–SiO_2. However, the influence of the TiO_2–SiO_2 was more pronounced, but still acceptable, after dyeing with higher concentrations (2 and 3% owf). In addition, in comparison to the CIE $L^*a^*b^*$ color values for the dyed cotton samples without TiO_2–SiO_2, all dyeings with different TiO_2–SiO_2 concentrations tended towards less red and less blue, which can be seen from a lower a^* and less negative $-b^*$. CIE $L^*a^*b^*$ coordinates for all dyeings also indicated that a better quality of color tone (higher h value) was obtained with reactive dyeing, combined with TiO_2–SiO_2.

Table 1
ATR-FTIR absorption bands at 668 cm^{-1} for cotton cellulose before and after dyeing with 0.5, 1.0 and 1.5% owf Bezaktiv Red S-3B 150, combined with TiO_2–SiO_2 concentration from 1 to 3% owf at 60, 80 and 100 °C of used dyeing temperatures.

	A_{668}/A_{1200}			
Cotton–blank	2.12			
Sample		A_{668}/A_{1200} Dyeing temperature		
Cotton dyed: conc. Bezaktiv Red S-3B 150	TiO_2 Conc.	60 °C	80 °C	100 °C
0.5%	–	2.15	2.20	2.16
	1.0%	2.50	3.03	2.71
	2.0%	2.73	3.35	2.75
	3.0%	2.86	3.42	3.07
1.0%	–	2.19	2.98	2.80
	1.0%	2.67	3.17	2.56
	2.0%	2.85	3.68	2.82
	3.0%	2.79	3.14	2.94
1.5%	–	2.18	2.98	2.68
	1.0%	2.88	3.18	2.49
	2.0%	2.82	2.75	2.53
	3.0%	2.89	3.05	2.72

3.4. UV protection performance of the cotton Bezaktiv Red S-3B 150, combined with TiO_2–SiO_2 dyed samples at different dye and TiO_2–SiO_2 concentrations, and dyeing temperatures

The UV-blocking mechanism of this technology is attributed to the electronic structure of the treatment: titania absorbs light with an energy that matches or exceeds its band gap energy, which is ultraviolet region at wavelengths <380 nm and reflects visible and IR rays.

As shown in Fig. 6, an incorporation of 1%, 2% and 3% owf of TiO_2–SiO_2 to the dyeing process greatly enhanced UV-shielding properties of the dyed cotton samples, compared to the dyed sample without the TiO_2–SiO_2 incorporation.

The UPF of a fabric depends on fiber content and weave, used dyes, finishing processes, the presence of additives, and should be between 40 and 50+ to categorize the clothing cotton fabric to fabrics with an excellent UV protection. Based on these criteria blank plane-wave cotton fabric with UPF rating 10 is classified as non-rateable fabrics with inadequate protection for outdoor wearers. After dyeing fabrics with Bezaktiv Red S-3B 150, UPF values were increased with increasing dye concentration. But even at concentration of 1.5% owf, UPF was only 25 (i.e. at 60 °C, the optimal dyeing temperature according to dye manufacturer) showing insufficient dye UV-absorbing ability. The TiO_2–SiO_2 bonding onto cotton fabrics led to a rise of UPF values up to the UPF rating of 50+, which

Table 2
CIELAB color coordinates and K/S values of Bezaktiv Red S-3B 150, combined with TiO_2–SiO_2 dyed cotton samples.

Sample	TiO_2–SiO_2 conc.	L^*	a^*	b^*	ΔE^*	C^*	h	K/S
Cotton–blank		94.27	4.41	−15.22		15.84	286.15	0.01
Cotton dyed: Bezaktiv Red S-3B 150 conc./dyeing temperature								
0.5%/60 °C	–	77.03	31.01	−19.83		36.81	327.41	0.47
	1.0%	78.46	29.22	−17.98	2.94	34.31	328.40	0.41
	2.0%	79.12	27.95	−17.40	4.43	32.93	328.10	0.37
	3.0%	79.70	26.72	−16.95	5.81	31.64	327.61	0.34
1.0%/60 °C	–	72.01	35.96	−17.34		39.92	334.25	0.78
	1.0%	72.35	35.07	−16.83	1.08	38.90	334.37	0.76
	2.0%	72.66	34.64	−15.73	2.18	38.05	335.58	0.73
	3.0%	72.76	34.21	−15.69	2.51	37.64	335.35	0.73
1.5%/60 °C	–	68.09	39.20	−15.76		42.25	338.10	1.13
	1.0%	69.36	39.52	−15.90	1.31	42.60	338.08	1.05
	2.0%	69.93	39.07	−15.49	1.86	42.03	338.37	1.00
	3.0%	70.30	37.10	−14.91	3.16	39.99	338.10	0.93
0.5%/80 °C	–	76.47	31.20	−18.83		36.44	328.88	0.50
	1.0%	77.83	29.66	−18.60	2.06	35.01	327.91	0.44
	2.0%	77.96	29.56	−18.64	2.22	34.94	327.76	0.41
	3.0%	78.56	28.71	−18.56	3.26	34.18	327.12	0.40
1.0%/80 °C	–	72.04	35.17	−17.48		39.28	333.57	0.76
	1.0%	72.67	34.53	−17.16	0.95	38.56	333.57	0.75
	2.0%	73.11	34.34	−16.73	1.54	38.19	334.03	0.71
	3.0%	73.40	34.04	−16.31	2.12	37.75	334.40	0.70
1.5%/80 °C	–	68.28	39.35	−15.89		42.44	338.00	1.12
	1.0%	68.37	39.24	−15.35	0.55	42.14	338.64	1.09
	2.0%	68.49	39.23	−15.19	0.74	42.07	338.83	1.09
	3.0%	68.87	38.93	−15.06	1.10	41.75	338.85	1.07
0.5%/100 °C	–	80.06	27.58	−19.22		33.62	325.12	0.34
	1.0%	81.17	26.29	−18.63	1.80	32.22	324.67	0.30
	2.0%	81.63	26.03	−17.11	3.05	31.15	326.68	0.30
	3.0%	81.76	26.00	−16.06	3.92	30.56	328.30	0.30
1.0%/100 °C	–	74.31	34.58	−18.11		39.03	332.36	0.60
	1.0%	74.88	34.01	−17.36	1.10	38.19	332.95	0.59
	2.0%	75.04	33.50	−16.97	1.73	37.55	333.13	0.58
	3.0%	75.24	32.90	−16.20	2.70	36.67	333.78	0.57
1.5%/100 °C	–	70.41	37.90	−16.58		41.37	336.37	0.93
	1.0%	71.30	36.83	−16.26	1.42	40.26	336.19	0.79
	2.0%	71.56	36.80	−16.12	1.65	40.17	336.34	0.76
	3.0%	71.94	36.38	−15.65	2.34	39.60	336.73	0.72

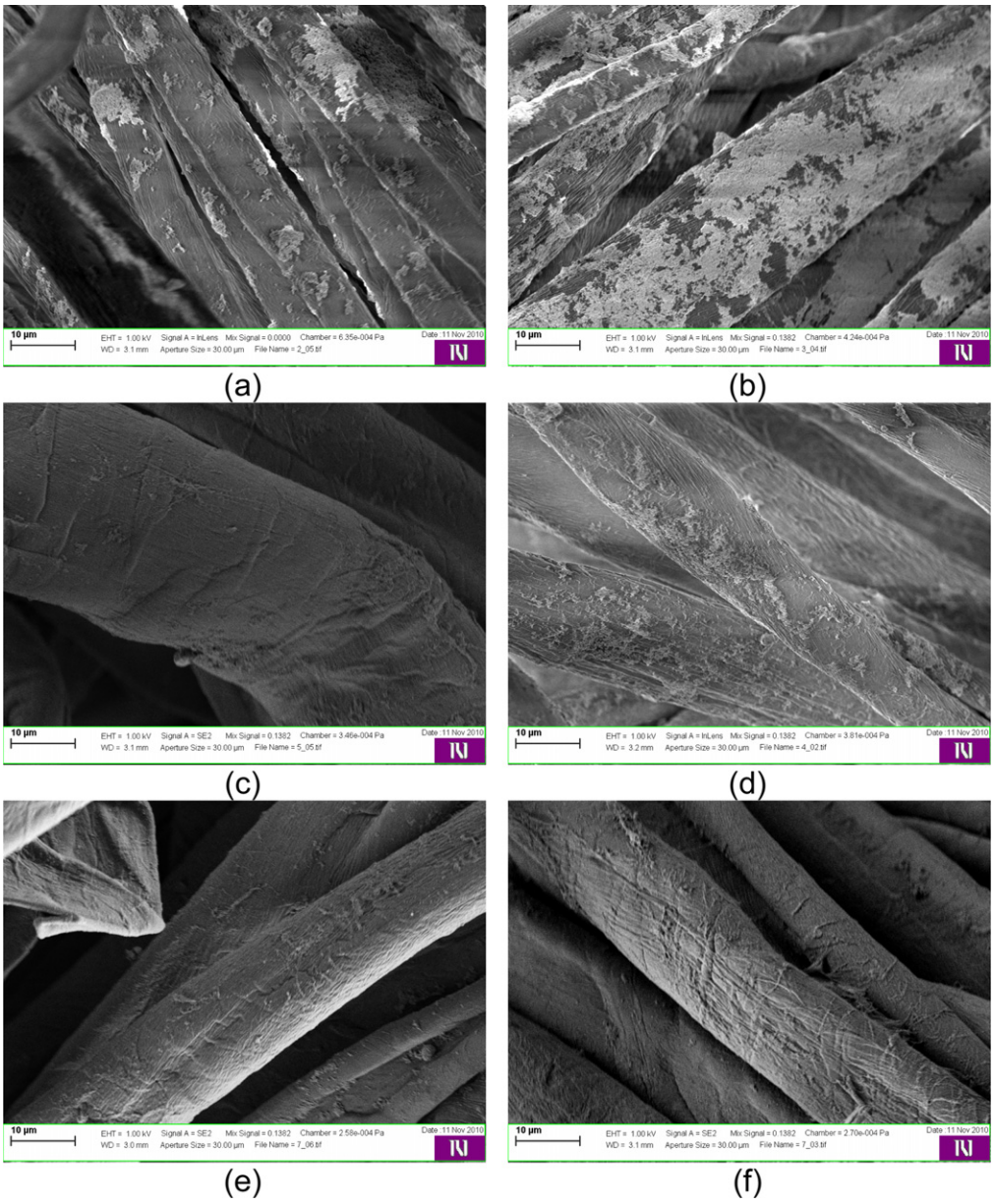

Fig. 5. SEM images of the 1% Bezaktiv Red S-3B 150 dyed cotton fibers at (a) 60 °C with 1% TiO_2–SiO_2, (b) 60 °C with 3% TiO_2–SiO_2, (c) 80 °C with 1% TiO_2–SiO_2, (d) 80 °C with 3% TiO_2–SiO_2, (e) 100 °C with 1% TiO_2–SiO_2 and (f) 100 °C with 3% TiO_2–SiO_2; taken at magnification of 15×10^3.

assigns the maximum UV protection. UPF values were improved by raising the TiO_2–SiO_2 concentration from 1 to 3% owf at all dyeing temperatures. Remarkable UPF values, i.e. 40–50+ were already achieved at 1% owf of used TiO_2–SiO_2, but using 2% owf enabled UPF values over 50 at all dyeing temperatures. Increasing TiO_2–SiO_2 concentration beyond 2% owf had practically a slight or no positive effect on the UV protection properties. Increased concentration of particles in dyeing baths facilitates forming an undesirable complex between dye molecules and particles according to their electrostatic interactions. This complex formation occurs in dye bath before the dye absorption. Therefore it can limit the dye diffusion. In fact the complex can block dye molecules in its structure. They can also deposit on the fabric surfaces and filter the other dye molecules and limit their diffusion. Moreover, they cannot strongly link to the fabrics and will be easily removed by the post process. As far as the changes in UPF values as a function of temperature, the obtained results disclose that with increasing the dyeing temperature from 60 °C to 80 °C increased both, UPF and *K*/*S*, values reflecting the positive impact of higher temperature on enhancing the swellability of the treated cotton fabrics as well as solubility of the reactive dye thereby opening the cellulose structure, enhancing the extent of penetration/fixation and diffusion of both the TiO_2–SiO_2 and reactive dye molecules. On the other hand, further temperature increasing up to 100 °C resulted in a decrease in the UV protection properties and *K*/*S* values, irrespective of the used dye and TiO_2–SiO_2 concentrations, which can be explained in terms of undesirable dye–particle complex formation and lower stability of the used dye (i.e. partial hydrolysis of the active chlorine atoms in the triazine ring) (Ojstršek et al., 2008) thereby resulting in a lower dye retention and fixation, i.e. lighter depth of shade (Table 2) with lower degree of UV-protection (Fig. 6).

3.5. Fabric surface characterization

Fiber surface morphology of the dyed cotton samples (1% owf Bezaktiv Red S-3B combined with 1% and 3% owf TiO_2–SiO_2) at

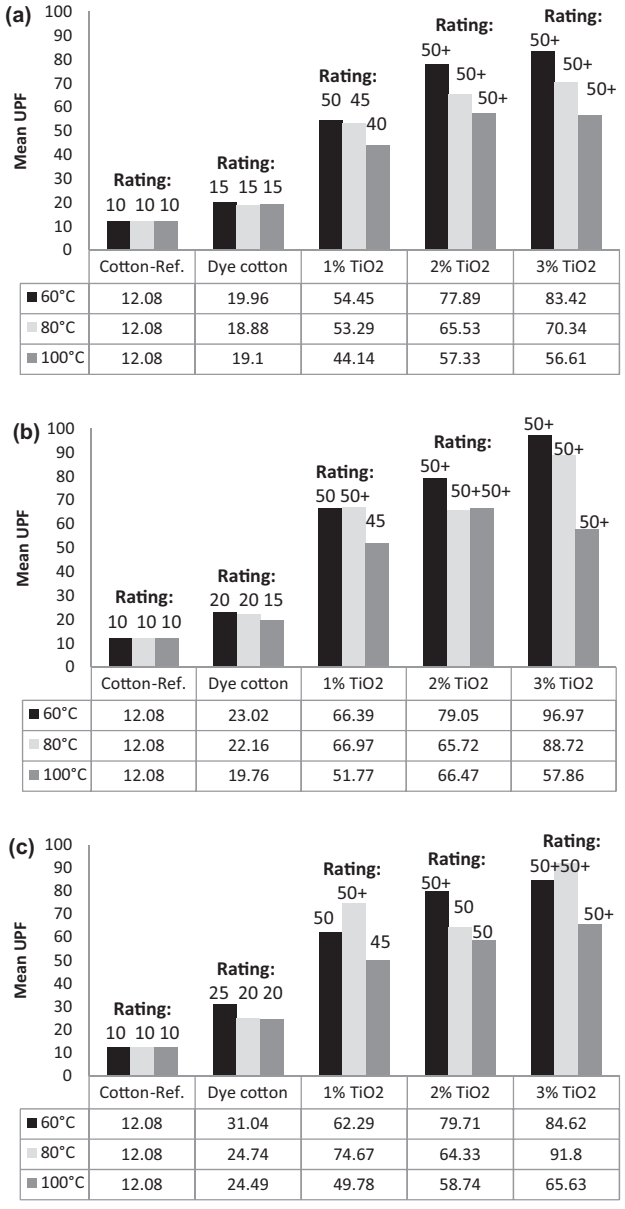

Fig. 6. Effect of TiO_2–SiO_2 concentration on obtained dyed cotton UPF at (a) 0.5%, (b) 1.0% and (c) 1.5% owf Bezaktiv Red S-3B 150 concentration.

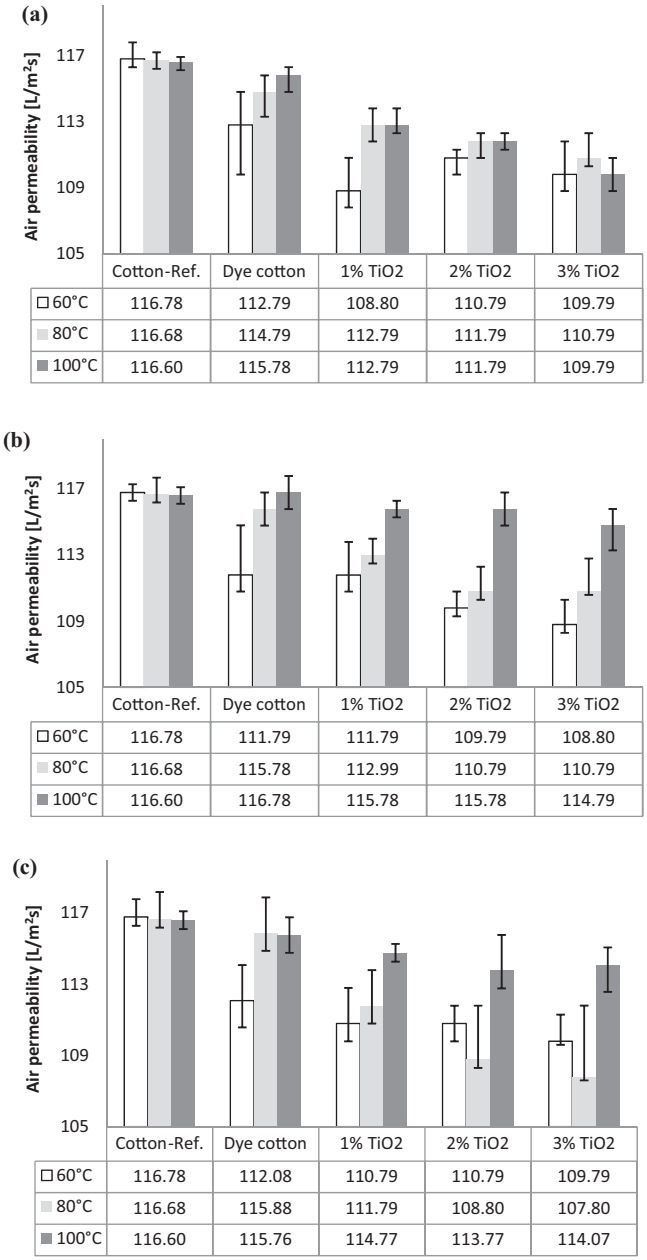

Fig. 7. Effect of TiO_2–SiO_2 concentration on obtained dyed cotton air permeability at (a) 0.5%, (b) 1.0% and (c) 1.5% owf Bezaktiv Red S-3B 150 concentration.

60 °C, 80 °C and 100 °C is presented in Fig. 5. Nanomodifications changed the surface of fibers; however, the three different dyeing temperatures lead to different coating morphologies. In the case of fibers dyeing at 60 °C (Fig. 5(a) and (b)), a non-uniform surface is obtained. Large aggregates or clusters of TiO_2–SiO_2 particles can be observed at concentration 1% owf TiO_2–SiO_2 (Fig. 5(a)) and larger aggregates at concentration 3% owf TiO_2–SiO_2 (Fig. 5(b)). With rising temperature up to 100 °C, the surface structure of the treated cotton fabric was smoother with higher coating homogeneity, indicating the formation of a uniform continuous layer (Fig. 5(e) and (f)). Because of the nano thickness, film is transparent and the difference in the color of the treated fabrics at 100 °C is the least distinctive (Table 2).

3.6. Air permeability

As is evident from Fig. 7, raising the temperature up to 100 °C brings a slight increase in the air permeabilities, which can also be attributed to cotton impurity removal in alkaline medium (Fakin & Ojstršek, 2008). Furthermore, decrease in the air permeabilities of the samples with increasing TiO_2–SiO_2 concentration from 1 to 3% owf was not significant. However, by increasing the temperature this effect has been compensated. In the case of samples treated at temperature of 60 °C possibly the sizes of agglomerated particles were so big that can block the fabric voids to some extent (Fig. 5). Therefore air permeability in these samples was decreased compared to other samples. However changes in air permeability of other samples were not statistically significant because of very small size of particles compared to fabric holes. Consequently, achieving sufficient UV protection, without affecting coloration process and obtained fabrics color is possible without any reduction in air permeability using the appropriate compound concentrations under optimal dyeing conditions.

3.7. Light fastness properties

To determine the actual UV protecting capability of SiO_2 layers on TiO_2, color fastnesses properties to light were determined. The Bezaktiv Red S-3B 150 photodegradation of the dyed cotton samples was evaluated by the standard ISO 150-B04 after 15 h of exposure of samples to the 1154 W/m^2 irradiation.

As shown in Table 3, after 15 h of UV irradiation, the cotton dyed samples without the addition of TiO_2–SiO_2 showed the same light fastnesses as the ones dyed with incorporated TiO_2–SiO_2 when comparing dyeings using equal dye concentrations. In other words, the protective SiO_2 coating effectively suppressed the photocatalytic activity of pure rutile TiO_2 while retained its UV-protective properties. Additionally, the presence of silica particles reduces the aggregation of the TiO_2 nanoparticles allowing extensive hydrogen bondings with cellulose (Veronovski, Andreozzi, et al., 2010; Veronovski, Sfiligoj-Smole, et al., 2010).

3.8. Washing durability

To examine the washing durability, the obtained dyeings were subjected to 1, 5, 10, and 15 wash cycles in Mathis Labomat machine and subjected to UPF test according to the above-mentioned testing method.

As shown in Table 4, increasing the wash cycle from 1 to 15 results in a reduction in UPF value by average 27% when dyed at 60 °C, 23% at 80 °C and 8% at 100 °C. The diminishing extent of decrease when dyed at 100 °C was most probably due to the homogeneous distribution of the lowest TiO_2–SiO_2 concentration, compared with samples dyed at 80 and 60 °C, where highest TiO_2–SiO_2 quantities with large aggregates or clusters were identified. Furthermore, at 100 °C the fiber swellability (opening up the fabric structure) is the highest and numerous accessible cellulose surface hydroxyls can enhance the diffusivity of the adsorbed TiO_2–SiO_2 nano particles and transfer of hydrogen from TiO_2–SiO_2 surface hydroxyls to the cellulose and its interaction with cellulose hydroxyls substantially increased laundering durability. On the other hand, the UV protection rating of excellent protection for the treated fabrics even after repeated 15 washing cycles is still maintained when using the combined dyeing process. Acceptable laundering durability can be attributed to enhanced bonding efficiency of the silica modified TiO_2 nanoparticles to the cotton fabric, as discussed earlier.

Table 3
Light fastness properties of Bezaktiv Red S-3B 150, combined with TiO_2–SiO_2 dyed cotton samples.

Sample		Light fastness (ISO 150-B04)
Cotton dyed: Bezaktiv Red S-3B 150 conc./dyeing temperature	TiO_2–SiO_2 conc.	
0.5%/60 °C	1.0%	4
	2.0%	4
	3.0%	4
	–	4
1.0%/60 °C	1.0%	4
	2.0%	4
	3.0%	4
	–	4
1.5%/60 °C	1.0%	4
	2.0%	3–4
	3.0%	3–4
	–	4
0.5%/80 °C	1.0%	4
	2.0%	4
	3.0%	4
	–	4
1.0%/80 °C	1.0%	4
	2.0%	4
	3.0%	4
	–	4
1.5%/80 °C	1.0%	4
	2.0%	4
	3.0%	4
	–	4
0.5%/100 °C	1.0%	3
	2.0%	3
	3.0%	3
	–	3
1.0%/100 °C	1.0%	3
	2.0%	3
	3.0%	3
	–	3
1.5%/100 °C	1.0%	3
	2.0%	3
	3.0%	3
	–	3

Table 4
Washing durability as UPF measurements after every five washing cycles.

Cotton dyed Samples		UPF											
Dye conc.	TiO_2–SiO_2 conc.	Washing cycles											
		1			5			10			15		
		Dyeing temperature											
		60 °C	80 °C	100 °C	60 °C	80 °C	100 °C	60 °C	80 °C	100 °C	60 °C	80 °C	100 °C
0.5%	–	19	18	17	17	17	16	16	15	12	16	15	13
	1.0%	53	53	44	54	46	42	47	41	40	44	40	41
	2.0%	71	60	55	59	45	49	54	46	48	52	45	48
	3.0%	78	66	53	80	52	47	73	51	45	65	52	46
1.0%	–	21	21	17	18	21	16	16	19	15	17	16	15
	1.0%	61	64	51	51	53	49	49	50	50	45	50	49
	2.0%	70	64	64	52	58	58	58	60	55	52	56	55
	3.0%	79	84	55	78	62	52	64	61	51	65	66	55
1.5%	–	29	23	22	24	23	22	24	19	19	23	18	19
	1.0%	59	70	48	50	54	45	49	51	44	46	45	43
	2.0%	70	61	55	53	59	53	47	55	53	48	51	54
	3.0%	78	89	62	74	82	59	53	62	55	53	59	54

4. Conclusions

TiO_2 in rutile crystalline structure, along with high UV capacity and low photoactivity, is shown to be an effective UV protector. The catalytic activity of TiO_2 nanoparticles was suppressed by coating them with insulating SiO_2 layer, using wet precipitation process. In addition to that, SiO_2 acts as an effective stabilizing and binding agent.

Incorporation of the synthesized SiO_2 surface treated TiO_2 nanoparticles in the reactive dyeing process resulted in the hydrogen bonding of the synthesized nanoparticles onto the cotton fabrics with imparted durable UV-protection even after 15 consecutive laundering cycles, and with minimal negligible impacts on coloration and air permeability performance.

SEM images revealed a uniform and continuous structure of the nano-scaled coating layer obtained at higher temperatures (i.e. 100 °C). Nano modification obtained at 100 °C also exhibited better durability, i.e. bonding, compared to ones obtained at 60 and 80 °C.

Finally, it can be concluded that the combined TiO_2–SiO_2-reactive dyeing is a very promising, simple and practical method for obtaining dyeings with outstanding protection properties against the harmful UV-radiation without effecting other performance properties.

Acknowledgement

This research has been supported by Slovenian Research Agency (project no. J2-2067).

References

Aiqin, H., Yanhong, Y., & Huawei, C. (2010). Uniform dispersion of silica nanoparticles on dyed cellulose surface by sol–gel method. *Carbohydrate Polymers*, *79*, 578–583.

Ajoy, K. S. (2004). An evaluation of UV protection imparted by cotton fabrics dyed with natural colorants. *BMC Dermatology*, *4*, 1–8.

Bozzi, A., Yuranova, T., & Kiwi, J. (2005). Self-cleaning of wool-polyamide and polyester textiles by TiO_2-rutile modification under daylight irradiation at ambient temperature. *Journal of Photochemistry and Photobiology A: Chemistry*, *172*, 27–34.

Božič, M., Díaz-González, M., Tzanov, T., Guebitz, G. M., & Kokol, V. (2009). Voltammetric monitoring of enzyme-mediated indigo reduction in the presence of various fibre materials. *Enzyme and Microbial Technology*, *45*, 317–323.

Ciolacu, D., Kovac, J., & Kokol, V. (2010). The effect of the cellulose-binding domain from *Clostridium cellulovorans* on the supramolecular structure of cellulose fibers. *Carbohydrate Research*, *345*, 621–630.

Cui, H. T., Zayat, M., Parejo, P. G., & Levy, D. (2008). Highly efficient inorganic transparent UV-protective thin-film coating by low temperature sol–gel procedure for application on heat-sensitive substrates. *Advanced Materials*, *20*, 65–68.

Dastjerdi, R., & Montazer, M. (2010). A review on the application of inorganic nanostructured materials in the modification of textiles: Focus on antimicrobial properties. *Colloids and Surfaces B: Biointerfaces*, *79*, 5–18.

Dastjerdi, R., Montazer, M., & Shahsavan, S. (2010). A novel technique for producing durable multifunctional textiles using nanocomposite coating. *Colloids and Surfaces B: Biointerfaces*, *81*, 32–41.

El Shafie, A., Fouda, M. M. G., & Hashem, M. (2009). One-step process for bioscouring and peracetic acid bleaching of cotton fabric. *Carbohydrate Polymers*, *78*, 302–308.

Fakin, D., & Ojstršek, A. (2008). Colour of flax fibres in regard to different pretreatment and dyeing processes. *Coloration Technology*, *124*, 216–222.

Hulleman, S. H. D., Hazendonk, J. M., & Dam, J. E. G. (1994). Determination of crystallinity in native cellulose from higher plants with diffuse reflectance Fourier transform infrared spectroscopy. *Carbohydrate Research*, *261*, 163–172.

Ojstršek, A., Doliška, A., & Fakin, D. (2008). Analysis of reactive dyestuffs and their hydrolysis by capillary electrophoresis. *Analytical Sciences*, *24*, 1581–1587.

Parks, G. A. (1965). The isoelectric points of solid oxides, solid hydroxides and aqueous hydroxo complex systems. *Chemical Reviews*, *65*, 177–198.

Reed, J. S. (1995). *Principles of ceramics processing* (2nd ed.). New York: Wiley.

Tavčer, P. F. (2010). Impregnation and exhaustion bleaching of cotton with peracetic acid. *Textile Research Journal*, *80*, 3–11.

Tomšič, B., Simončič, B., Orel, B., Černe, L., Tavčer, P. F., Zorko, M., et al. (2008). Sol–gel coating of cellulose fibres with antimicrobial and repellent properties. *Journal of Sol–Gel Science and Technology*, *47*, 44–57.

Veronovski, N., Andreozzi, P., La Mesa, C., & Sfiligoj-Smole, M. (2010). Stable TiO_2 dispersions for nanocoating preparation. *Surface & Coatings Technology*, *204*, 1445–1451.

Veronovski, N., Hribernik, S., Andreozzi, P., & Sfiligoj-Smole, M. (2009). Homogeneous self-cleaning coatings on cellulose materials derived from TIP/TiO_2 P25. *Fibers and Polymers*, *10*, 716–723.

Veronovski, N., Sfiligoj-Smole, M., & Viota, J. L. (2010). Characterization of TiO_2/TiO_2–SiO_2 coated cellulose textiles. *Textile Research Journal*, *80*, 55–62.

Veronovski, N., Verhovšek, D., & Selišnik, A. (2011). *Oplaščevanje rutilnih nanodelcev TiO_2 v suspenziji s hidratiziranim SiO_2 in Al_2O_3*. Slovenian Patent Application no. P-201000397.

Viravathana, P., & Marr, D. W. M. (2000). Optical trapping of titania/silica core–shell colloidal particles. *Journal of Colloid and Interface Science*, *221*, 301–307.

Wang, Q., & Hauser, P. J. (2010). Developing a novel UV protection process for cotton based on layer-by-layer self-assembly. *Carbohydrate Polymers*, *81*, 491–496.

Xin, J. H., Daoud, W. A., & Kong, Y. Y. (2004). A new approach to UV-blocking treatment for cotton fabrics. *Textile Research Journal*, *74*, 97–100.

Yang, H. Y., Zhu, S. K., & Pan, N. (2004). Studying the mechanisms of titanium dioxide as ultraviolet blocking additive for films and fabrics by an improved scheme. *Journal of Applied Polymer Science*, *92*, 3201–3210.

Zhang, Y., Wu, Y., Chen, M., & Wu, L. (2010). Fabrication method of TiO_2–SiO_2 hybrid capsules and their UV-protective property. *Colloids and Surfaces A: Physicochemical and Engineering Aspects*, *353*, 216–225.